August 18, 2015

South Fork Crooked River

Topobathymetric LiDAR Technical Data Report

Oregon LiDAR Consortium
Oregon Department of Geology and Mineral Industries
800 NE Oregon Street #28, Suite 985
Portland, OR 97232
PH: 202-423-5089

QSI Environmental
517 SW 2nd St., Suite 400
Corvallis, OR 97333
PH: 541-752-1204

TABLE OF CONTENTS

Cover Photo: View looking southeast over the Crooked River located at the southern tip of the AOI. The image was created from the gridded LiDAR surface draped with National Agriculture Imagery Program (NAIP) imagery and overlaid with the 3D LiDAR point cloud.

INTRODUCTION

This photo taken by QSI acquisition staff shows a view of the South Fork Crooked River landscape.

In May 2014, Quantum Spatial (QSI) was contracted by the Oregon LiDAR Consortium (OLC) to collect topobathymetric Light Detection and Ranging (LiDAR) data in the spring of 2014 for the South Fork Crooked River site in central Oregon. Initial acquisition of the South Fork Crooked River project was completed in the spring of 2014, but bathymetric data collection was determined to be unsuccessful due to widespread algal blooms impeding laser penetration. Acquisition was then scheduled for the following calendar year during early spring 2015. Algal blooms continued to be a factor; however increased bathymetric coverage was achieved. Traditional near-infrared (NIR) LiDAR was fully integrated with Green wavelength return data (bathymetric) in order to provide seamless and complete project mapping. In addition to the topobathymetric area of interest, an additional adjoining area of interest was also collected with NIR LiDAR only. Data were collected to aid OLC in assessing the topographic and geophysical properties (channel morphology and topobathymetric surface) of the study area.

This report accompanies the delivered 2015 LiDAR data and documents contract specifications, data acquisition procedures, processing methods, and analysis of the final dataset including LiDAR accuracy and density. Acquisition dates and acreage are shown in Table 1, a complete list of contracted deliverables provided to OLC is shown in Table 2, and the project extent is shown in Figure 1.

Table 1: Acquisition dates, acreage, and data types collected on the South Fork Crooked River site

Project Site	Total Acres	Acquisition Dates	Data Type
South Fork Crooked River	776	04/17/2015	NIR LiDAR only AOI
	5,420	04/16/2015 - 04/17/2015	Topobathymetric LiDAR AOI

Deliverable Products

Table 2: Products delivered to OLC for the South Fork Crooked River site

South Fork Crooked River Products Projection: Oregon Statewide Lambert Horizontal Datum: NAD83 (2011) Vertical Datum: NAVD88 (GEOID12A) Units: International Feet	
Points	LAS v 1.2 • Topobathymetric Integrated All Returns with RGB Values Assigned • NIR AOI All Returns with RGB Values Assigned
Rasters	3.0 Foot ESRI Grids • Topobathymetric Bare Earth Model • NIR AOI Bare Earth Model • Highest Hit Model • Ground Density Raster 1.5 Foot GeoTiffs • Green Wavelength Intensity Images (ʎ = 532nm) • NIR Wavelength Intensity Images (ʎ = 1,064nm) • NIR AOI Intensity Images
Vectors	Shapefiles (*.shp) • Contracted and Buffered Site Boundaries • LiDAR Tile Indices • DEM Tile Indices • Water's Edge Polygon • Bathymetric Confidence Polygon • Flightline Trajectories (projected in UTM 10N) • Ground Control Point Data (projected in UTM 10N)

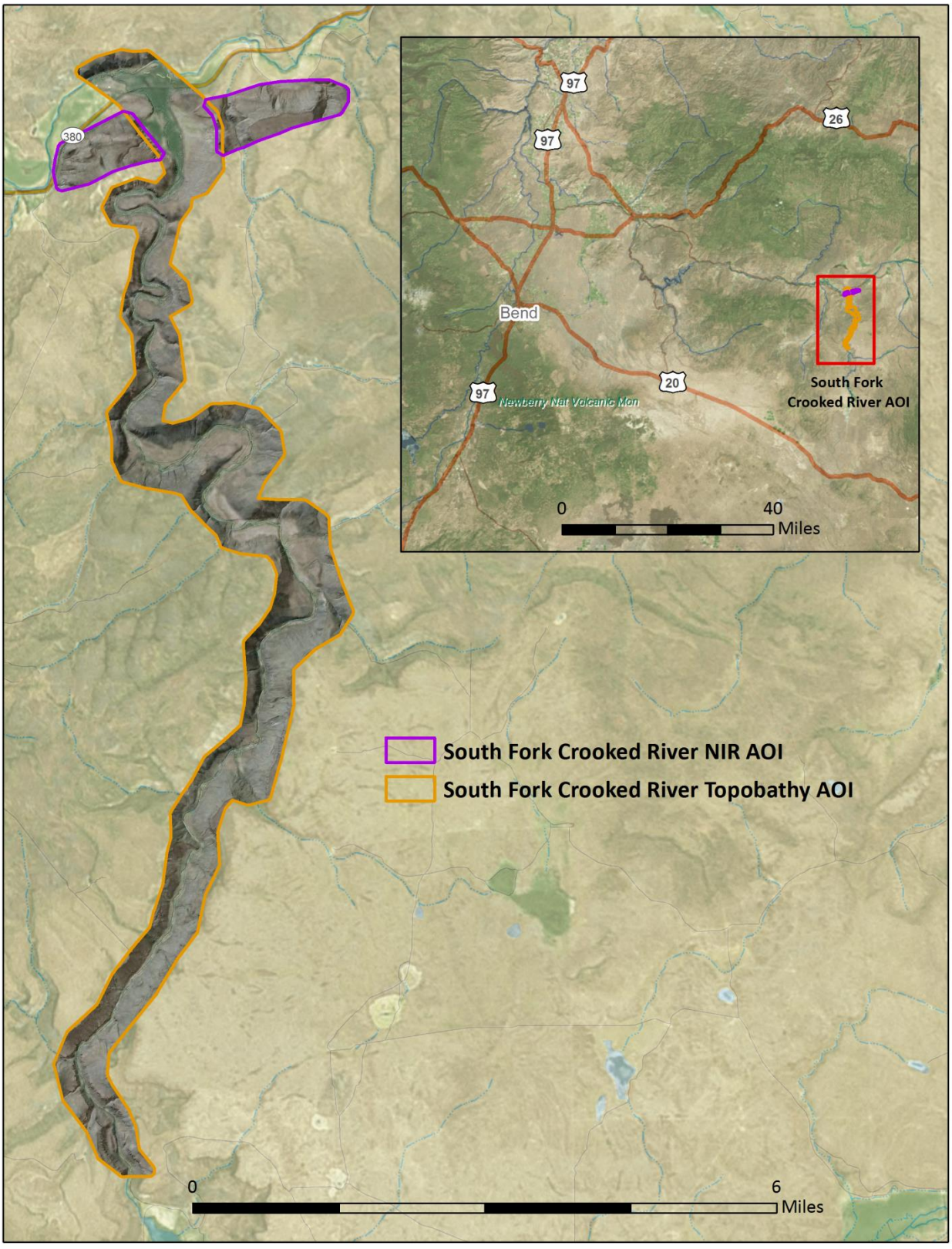

Figure 1: Location map of the South Fork Crooked River site in Oregon

QSI's Cessna Caravan

Sensor Selection: the Riegl VQ-820-G

The Riegl VQ-820-G was selected as the hydrographic airborne laser scanner for the South Fork Crooked River topobathymetric project based on fulfillment of several considerations deemed necessary for effective mapping of the project site. A high repetition pulse rate, high scanning speed, small laser footprint, and wide field of view allow for seamless collection of high resolution data of both topographic and bathymetric surfaces. A short laser pulse length allows for discrimination of underwater surface expression in shallow water, critical to shallow and dynamic environments such as the South Fork Crooked River. Sensor specifications and settings for the South Fork Crooked River acquisition are displayed in Table 6.

Planning

In preparation for data collection, QSI reviewed the project area and developed a specialized flight plan to ensure complete coverage of the South Fork Crooked River Topobathymetric LiDAR study area at the target point density of ≥5.0 points/m^2 for green LiDAR returns, and ≥8.0 points/m^2 for NIR LiDAR returns. Acquisition parameters including orientation relative to terrain, flight altitude, pulse rate, scan angle, and ground speed were adapted to optimize flight paths and flight times while meeting all contract specifications.

Factors such as satellite constellation availability and weather windows must be considered during the planning stage. Any weather hazards or conditions affecting the flight were continuously monitored due to their potential impact on the daily success of airborne and ground operations. In addition, logistical considerations including private property access and potential air space restrictions, river flow rates (Figure 2 and Figure 3), and water clarity were reviewed.

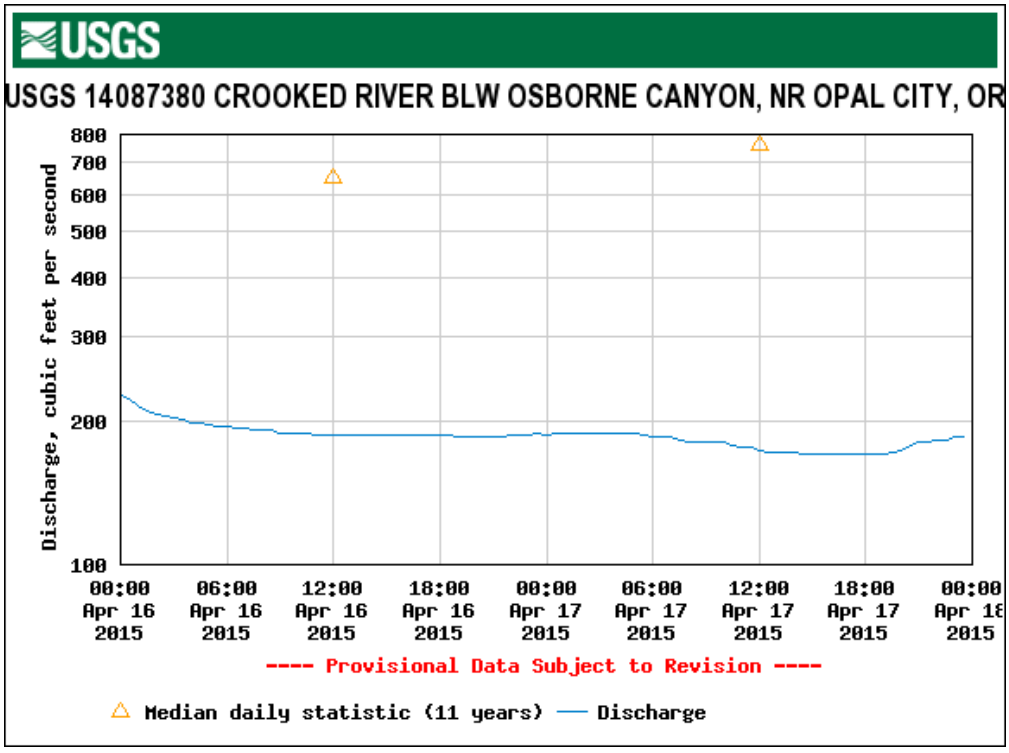

Figure 2: Flow rates (cfs) of the South Fork Crooked River at USGS Gauge Station 14087380 at the time of LiDAR acquisition, April 16 – 17, 2015.

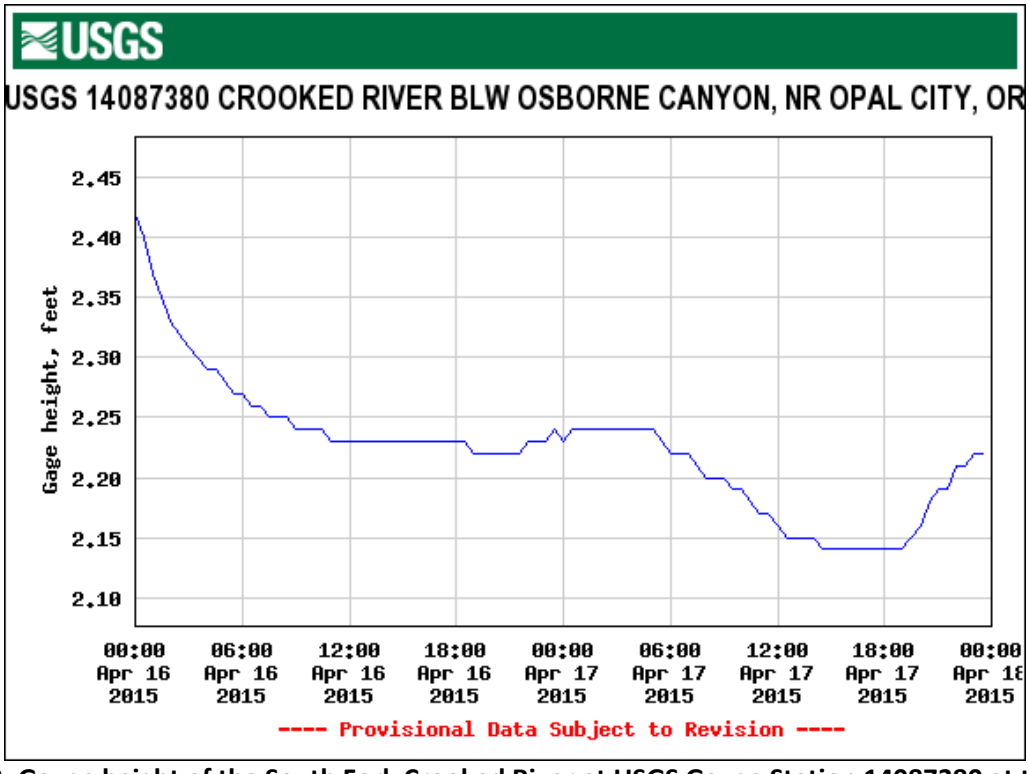

Figure 3: Gauge height of the South Fork Crooked River at USGS Gauge Station 14087380 at the time of LiDAR acquisition, April 16 – 17, 2015.

These photos taken by QSI acquisition staff display water clarity conditions and algal blooms at two locations within the South Fork Crooked River site.

LiDAR Airborne Survey

The NIR only AOI was accomplished using a using a Leica ALS70 system and the topobathymetric LiDAR survey was accomplished using a Leica ALS70 system dual mounted with a Riegl VQ-820-G topobathymetric sensor in a Cessna 208B Caravan. The Riegl VQ-820-G uses a green wavelength (ʎ=532 nm) laser that is capable of collecting high resolution vegetation and topography data, as well as penetrating the water surface with minimal spectral absorption by water. The recorded waveform enables range measurements for all discernible targets for a given pulse. The Leica ALS70 and Riegl laser systems can record unlimited range measurements (returns) per pulse, but typically do not record more than 5 returns per pulse. It is not uncommon for some types of surfaces (e.g., dense vegetation or water) to return fewer pulses to the LiDAR sensors than the lasers originally emitted. The discrepancy between first return and overall delivered density will vary depending on terrain, land cover, water clarity, and depth. All discernible laser returns were processed for the output dataset. Table 3 summarizes the settings used to yield an average pulse density of ≥8 pulses/m^2 in the NIR only AOI and ≥5 pulses/m^2 for the topobathymetric AOI.

Table 3: LiDAR specifications and survey settings

LiDAR Survey Settings & Specifications			
	Leica ALS70 (Co-Acquired)	**Riegl VQ-820-G**	**Leica ALS70 (NIR Only)**
Acquisition Dates	April 16-17, 2015	April 16-17, 2015	April 17, 2015
Aircraft Used	Cessna 208B	Cessna 208B	Cessna 208B
Survey Altitude (AGL)	600 m	600 m	1,400 m
Target Pulse Rate	300 kHz	284 kHz	190 kHz
Pulse Mode	Single Pulse in Air (SPiA)	Single Pulse in Air (SPiA)	Single Pulse in Air (SPiA)
Laser Pulse Diameter	15 cm	60 cm	32 cm
Mirror Scan Rate	40 Hz	50.8 Hz	40 Hz
Field of View	30°	44°	30°
GPS Baselines	≤13 nm	≤13 nm	≤13 nm
GPS PDOP	≤3.0	≤3.0	≤3.0
GPS Satellite Constellation	≥6	≥6	≥6
Maximum Returns	Unlimited, but typically not more than 5	Unlimited, but typically not more than 5	Unlimited, but typically not more than 5
Intensity	8-bit, scaled to 16-bit	16-bit	8-bit
Resolution/Density	Average 8 pulses/m^2	Average 5 pulses/m^2	Average 8 pulses/m^2
Accuracy	$RMSE_Z$ ≤ 15 cm	$RMSE_Z$ ≤ 30 cm	$RMSE_Z$ ≤ 15 cm

All areas were surveyed with an opposing flight line side-lap of ≥50% (≥100% overlap) in order to reduce laser shadowing and increase surface laser painting. To accurately solve for laser point position (geographic coordinates x, y and z), the positional coordinates of the airborne sensor and the attitude of the aircraft were recorded continuously throughout the LiDAR data collection mission. Position of the aircraft was measured twice per second (2 Hz) by an onboard differential GPS unit, and aircraft attitude was measured 200 times per second (200 Hz) as pitch, roll and yaw (heading) from an onboard inertial measurement unit (IMU). To allow for post-processing correction and calibration, aircraft and sensor position and attitude data are indexed by GPS time.

Ground Control

Ground control surveys, including monumentation and ground survey points (GSPs), were conducted to support the airborne acquisition. Ground control data were used to geospatially correct the aircraft positional coordinate data and to perform quality assurance checks on final LiDAR data.

QSI-Established Monument

Monumentation

The spatial configuration of ground survey monuments provided redundant control within 13 nautical miles of the mission areas for LiDAR flights. Monuments were also used for collection of ground survey points using real time kinematic (RTK) and post processed kinematic (PPK) survey techniques.

Monument locations were selected with consideration for satellite visibility, field crew safety, and optimal location for GSP coverage. QSI established three new monuments for the South Fork Crooked River LiDAR project (Table 4, Figure 4). New monumentation was set using 5/8" x 30" rebar topped with stamped 2" aluminum caps. QSI's professional land surveyor, Christopher Glantz (OR PLS #83648) oversaw and certified the establishment of all monuments.

Table 4: Monuments established for the South Fork Crooked River acquisition. Coordinates are on the NAD83 (2011) datum, epoch 2010.00

Monument ID	Latitude	Longitude	Ellipsoid (meters)
SF_CROOK_01	44° 03' 52.05940"	-120° 01' 22.08327"	1252.114
SF_CROOK_02	44° 03' 27.18145"	-120° 00' 37.81200"	1217.567
SF_CROOK_03	44° 05' 57.77359"	-120° 02' 46.85023"	1089.034

To correct the continuously recorded onboard measurements of the aircraft position, QSI concurrently conducted multiple static Global Navigation Satellite System (GNSS) ground surveys (1 Hz recording frequency) over each monument. During post-processing, the static GPS data were triangulated with nearby Continuously Operating Reference Stations (CORS) using the Online Positioning User Service (OPUS[1]) for precise positioning. Multiple independent sessions over the same monument were processed to confirm antenna height measurements and to refine position accuracy.

Monuments were established according to the national standard for geodetic control networks, as specified in the Federal Geographic Data Committee (FGDC) Geospatial Positioning Accuracy Standards for geodetic networks.[2] This standard provides guidelines for classification of monument quality at the 95% confidence interval as a basis for comparing the quality of one control network to another. The monument rating for this project is shown in Table 5.

[1] OPUS is a free service provided by the National Geodetic Survey to process corrected monument positions. http://www.ngs.noaa.gov/OPUS.

[2] Federal Geographic Data Committee, Geospatial Positioning Accuracy Standards (FGDC-STD-007.2-1998). Part 2: Standards for Geodetic Networks, Table 2.1, page 2-3. http://www.fgdc.gov/standards/projects/FGDC-standards-projects/accuracy/part2/chapter2

Table 5: Federal Geographic Data Committee monument rating for network accuracy

Direction	Rating
1.96 * St Dev $_{NE}$:	0.020 m
1.96 * St Dev $_{z}$:	0.020 m

For the South Fork Crooked River LiDAR project, the monument coordinates contributed no more than 2.8 cm of positional error to the geolocation of the final ground survey points and LiDAR, with 95% confidence.

Ground Survey Points (GSPs)

Ground survey points were collected using real time kinematic and post-processed kinematic (PPK) survey techniques. A Trimble R7 base unit was positioned at a nearby monument to broadcast a kinematic correction to a roving Trimble R8 GNSS receiver. All GSP measurements were made during periods with a Position Dilution of Precision (PDOP) of ≤ 3.0 with at least six satellites in view of the stationary and roving receivers. When collecting RTK and PPK data, the rover records data while stationary for five seconds, then calculates the pseudorange position using at least three one-second epochs. Relative errors for any GSP position must be less than 1.5 cm horizontal and 2.0 cm vertical in order to be accepted. See Table 6 for Trimble unit specifications.

GSPs were collected in areas where good satellite visibility was achieved on paved roads and other hard surfaces such as gravel or packed dirt roads. GSP measurements were not taken on highly reflective surfaces such as center line stripes or lane markings on roads due to the increased noise seen in the laser returns over these surfaces. GSPs were collected within as many flightlines as possible; however the distribution of GSPs depended on ground access constraints and monument locations and may not be equitably distributed throughout the study area (Figure 4).

Table 6: Trimble equipment identification

Receiver Model	Antenna	OPUS Antenna ID	Use
Trimble R7 GNSS	Zephyr GNSS Geodetic Model 2 RoHS	TRM57971.00	Static
Trimble R8	Integrated Antenna R8 Model 2	TRM_R8_GNSS	Rover

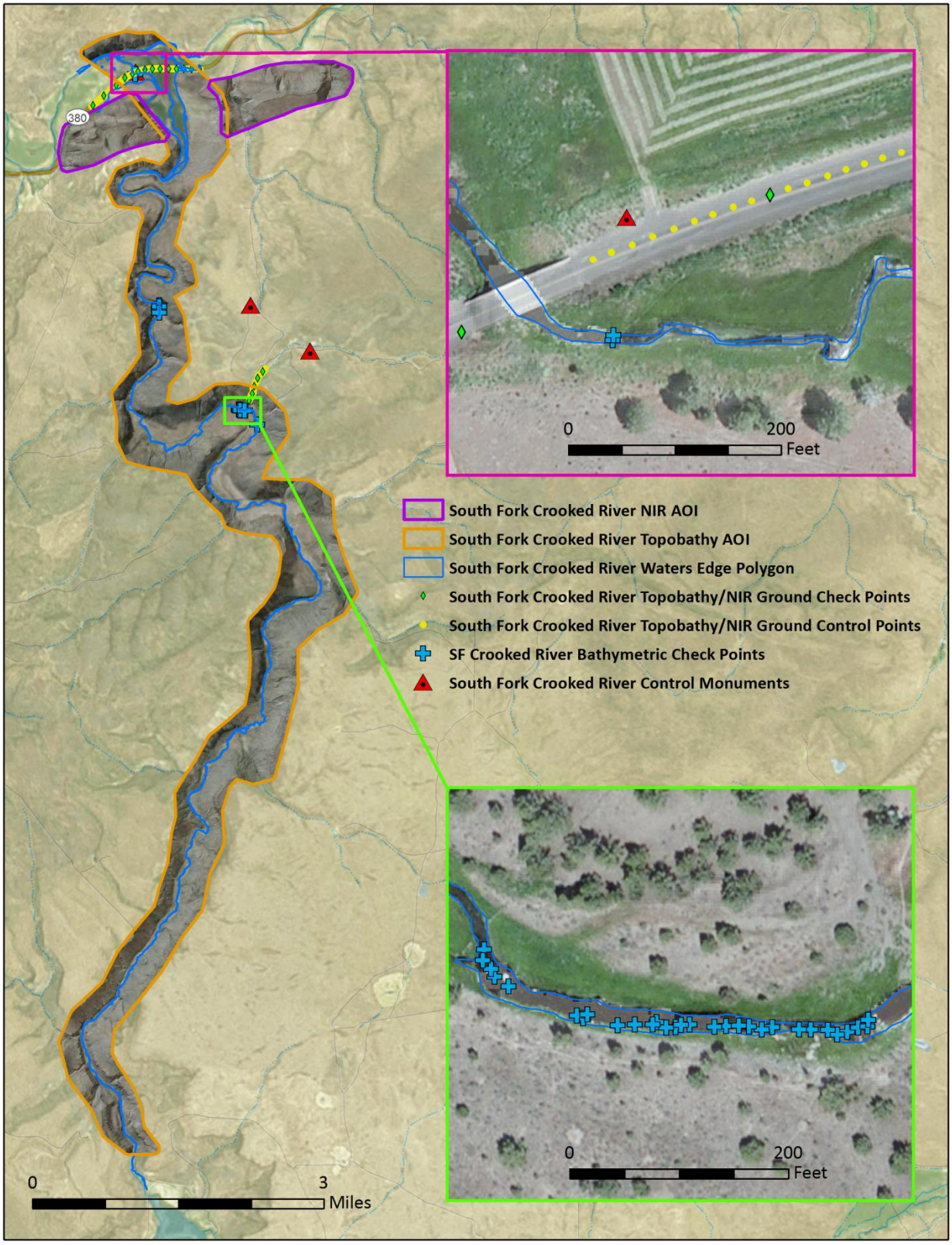

Figure 4: Ground control location map

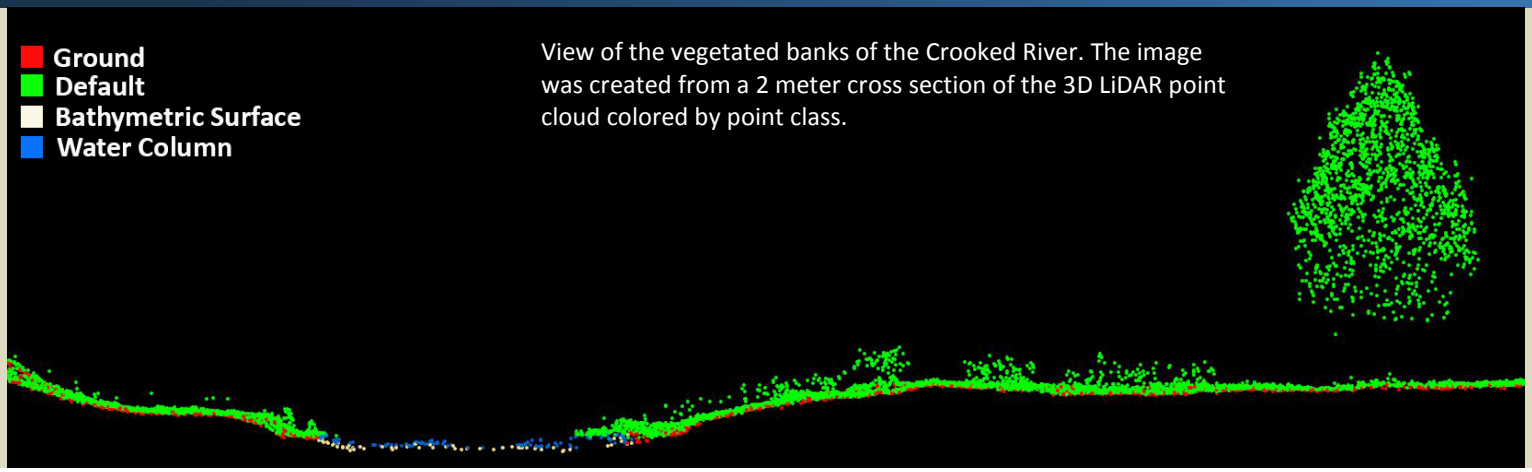

View of the vegetated banks of the Crooked River. The image was created from a 2 meter cross section of the 3D LiDAR point cloud colored by point class.

Topobathymetric LiDAR Data

Upon completion of data acquisition, QSI processing staff initiated a suite of automated and manual techniques to process the data into the requested deliverables. Processing tasks included GPS control computations, smoothed best estimate trajectory (SBET) calculations, kinematic corrections, calculation of laser point position, sensor and data calibration for optimal relative and absolute accuracy, and LiDAR point classification (Table 7). Riegl's RiProcess software was used to facilitate bathymetric return processing. Once bathymetric points were differentiated, they were spatially corrected for refraction through the water column based on the angle of incidence of the laser. QSI refracted water column points using QSI's proprietary LAS processing software, LAS Monkey. The resulting point cloud data were classified using both manual and automated techniques. Processing methodologies were tailored for the landscape. Brief descriptions of these tasks are shown in Table 8.

Table 7: ASPRS LAS classification standards applied to the South Fork Crooked River dataset

Classification Number	Classification Name	Classification Description
1	Default/Unclassified	Laser returns that are not included in the ground class, composed of vegetation and man-made structures
2	Ground	Laser returns that are determined to be ground or bathymetric bottom using automated and manual cleaning algorithms
9	Water Surface	NIR Laser returns that are determined to be water using automated and manual cleaning algorithms.
25	Water Column	Refracted Riegl sensor returns that are determined to be water using automated and manual cleaning algorithms.

Table 8: LiDAR processing workflow

LiDAR Processing Step	Software Used
Resolve kinematic corrections for aircraft position data using kinematic aircraft GPS and static ground GPS data. Develop a smoothed best estimate of trajectory (SBET) file that blends post-processed aircraft position with sensor head position and attitude recorded throughout the survey.	IPAS TC v.3.1 Waypoint Inertial Explorer v.8.5 POSPac MMS v6.2
Calculate laser point position by associating SBET position to each laser point return time, scan angle, intensity, etc. Create raw laser point cloud data for the entire survey in *.las (ASPRS v. 1.2) format. Convert data to orthometric elevations by applying a geoid correction.	ALS Post Processing Software v.2.75 RiProcess v1.6.4 TerraMatch v.15
Import raw laser points into manageable blocks (less than 500 MB) to perform manual relative accuracy calibration and filter erroneous points. Classify ground points for individual flight lines.	TerraScan v.15
Using ground classified points per each flight line, test the relative accuracy. Perform automated line-to-line calibrations for system attitude parameters (pitch, roll, heading), mirror flex (scale) and GPS/IMU drift. Calculate calibrations on ground classified points from paired flight lines and apply results to all points in a flight line. Use every flight line for relative accuracy calibration.	TerraMatch v.15 RiProcess v1.6.4
Apply refraction correction to all subsurface returns.	LAS Monkey
Classify resulting data to ground and other client designated ASPRS classifications (Table 7). Assess statistical absolute accuracy via direct comparisons of ground classified points to ground control survey data.	TerraScan v.15 TerraModeler v.15
Generate bare earth models as triangulated surfaces. Generate highest hit models as a surface expression of all classified points. Export all surface models as ESRI GRIDs at a 3.0 foot pixel resolution.	TerraScan v.15 TerraModeler v.15 ArcMap v. 10.1
Rescale intensity values to 16-bit and export intensity images as GeoTIFFs at a 1.5 foot pixel resolution.	TerraScan v.15 TerraModeler v.15 ArcMap v. 10.1

Bathymetric Refraction

The water surface model used for refraction is generated using NIR points within the breaklines defining the water's edge. Points are filtered and edited to obtain the most accurate representation of the water surface and are used to create a water surface model TIN. A TIN model is preferable to a raster based water surface model to obtain the most accurate angle of incidence during refraction. The refraction processing is done using Las Monkey; QSI's proprietary LiDAR processing tool. After refraction, the points are compared against bathymetric control points to assess accuracy.

LiDAR Derived Products

Because hydrographic laser scanners penetrate the water surface to map submerged topography, this affects how the data should be processed and presented in derived products from the LiDAR point cloud. The following discusses certain derived products that vary from the traditional (NIR) specification and delivery format.

Topobathymetric DEMs

Bathymetric bottom returns can be limited by depth, water clarity, and bottom surface reflectivity. Water clarity and turbidity affect the depth penetration capability of the green wavelength laser with returning laser energy diminishing by scattering throughout the water column. Additionally, the bottom surface must be reflective enough to return remaining laser energy back to the sensor at a detectable level. Although the predicted depth penetration range of the Riegl VQ-820-G sensor is one Secchi depth on brightly reflective surfaces, it is not unexpected to have no bathymetric bottom returns in turbid or non-reflective areas.

As a result, creating digital elevation models (DEMs) presents a challenge with respect to interpolation of areas with no returns. Traditional DEMs are "unclipped", meaning areas lacking ground returns are interpolated from neighboring ground returns (or breaklines in the case of hydro-flattening), with the assumption that the interpolation is close to reality. In bathymetric modeling, these assumptions are prone to error because a lack of bathymetric returns can indicate a change in elevation that the laser can no longer map due to increased depths. The resulting void areas may suggest greater depths, rather than similar elevations from neighboring bathymetric bottom returns. Therefore, QSI created a water polygon with bathymetric coverage to delineate areas with successfully mapped bathymetry (See Results & Discussion below). This shapefile was used to control the extent of the delivered topobathymetric model to avoid false triangulation (interpolation from TIN'ing) across areas in the water with no bathymetric returns.

Intensity Images

In traditional NIR LiDAR, intensity images are often made using first return information. For bathymetric LiDAR however, it is most often the last returns that capture features of interest below the water's surface. Therefore, a first return intensity image would display intensity information of the water's surface, obscuring the features of interest below.

With bathymetric LiDAR a more detailed and informative intensity image can be created by using all or selected point classes, rather than relying on return number alone. If intensity information of the bathymetry is the primary goal, water surface and water column points can be excluded. However, water surface and water column points often contain potentially useful information about turbidity and submerged but unclassified features such as vegetation. For the South Fork Crooked River project, QSI created one set of intensity images from NIR laser first returns, as well as one set of intensity images

from green laser returns. Green laser intensity images were created using first returns over terrestrial areas only, as well as all water column and bathymetric bottom points in order to display more detail in intensity values (Figure 5).

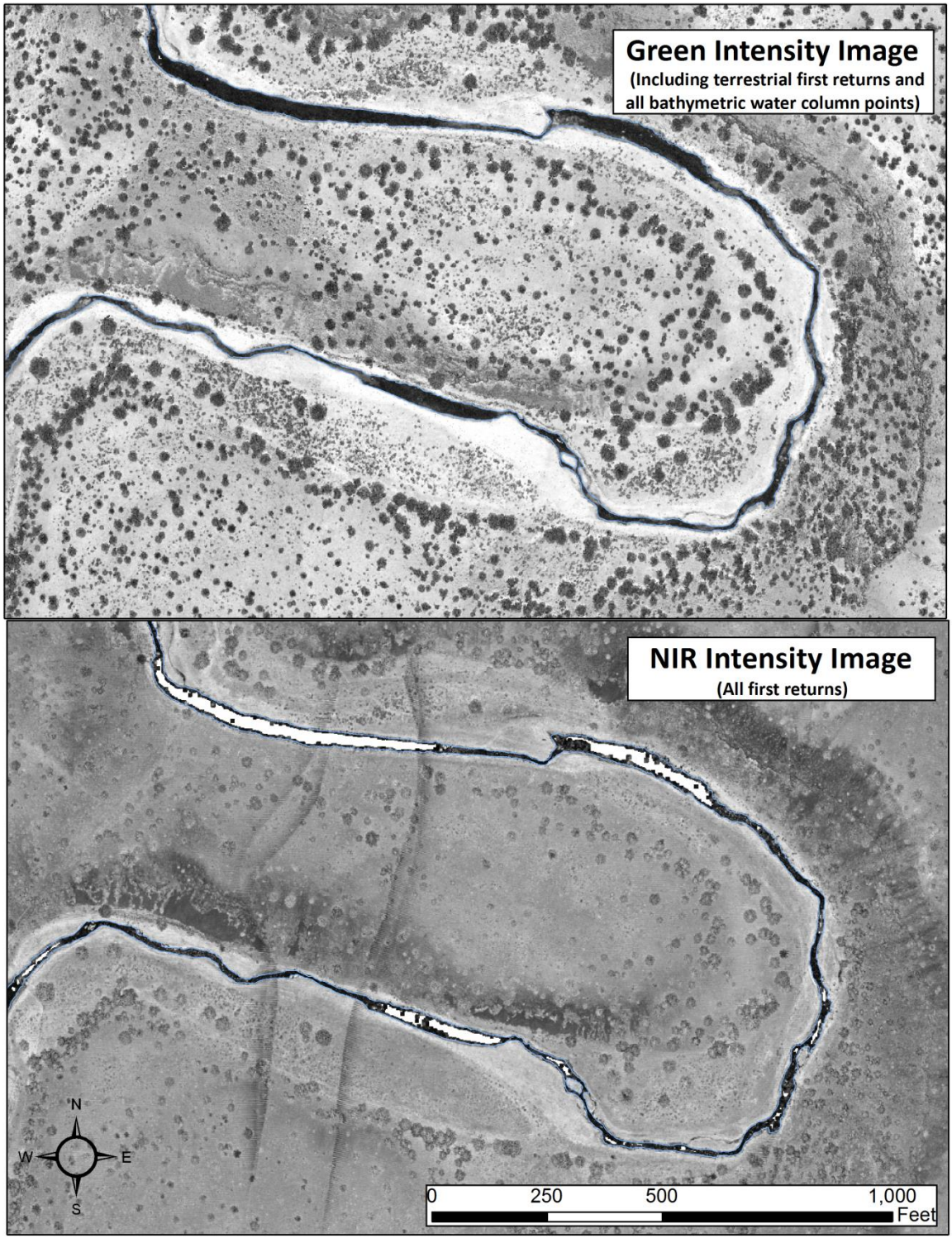

Figure 5: A comparison of Intensity Images from Green and NIR returns in the SF Crooked River project

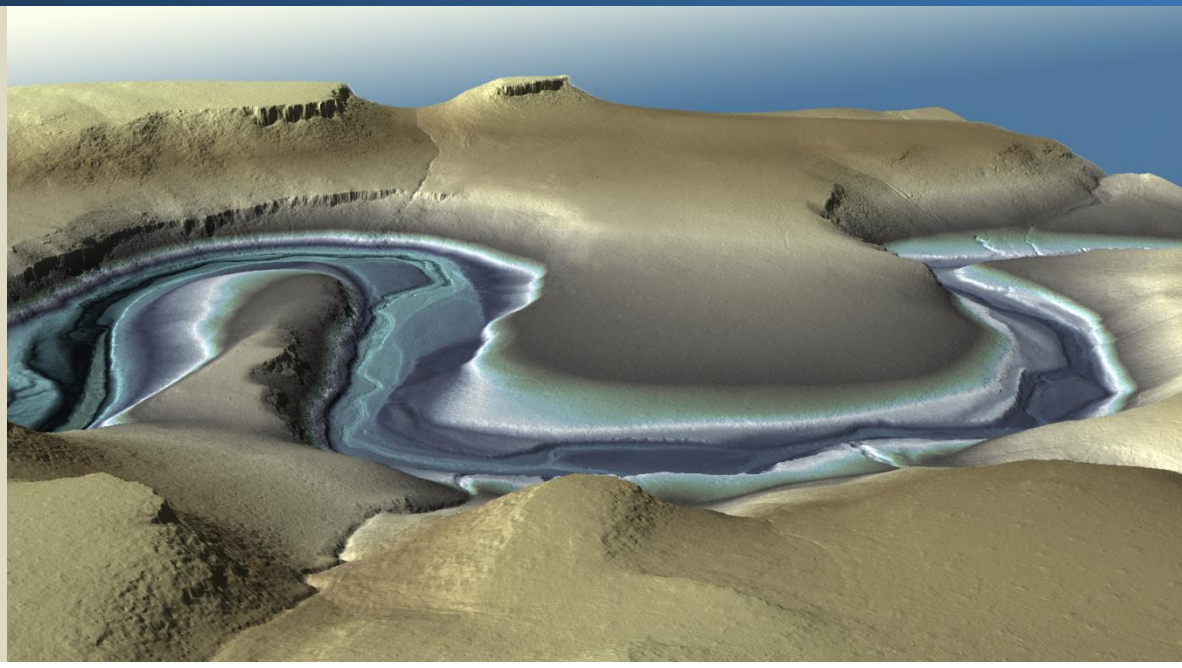

This image displays a view looking west over the South Fork Crooked River. The image was created from the gridded topobathymetric LiDAR surface colored by elevation.

Bathymetric LiDAR

An underlying principle for collecting hydrographic LiDAR data is to survey areas that can be difficult to collect with other methods, such as multi-beam sonar. In order to determine the capability and effectiveness of the bathymetric LiDAR, several parameters were considered; depth penetrations below the water surface, bathymetric return density, and spatial accuracy.

Mapped Bathymetry and Depth Penetration

The specified depth penetration range of the Riegl VQ-820-G sensor is one secchi depth; therefore, bathymetry data below one secchi depth at the time of acquisition is not to be expected. To assist in evaluating performance results of the sensor, a polygon layer was created to delineate areas where bathymetry was successfully mapped.

This shapefile was used to control the extent of the delivered topobathymetric model to avoid false triangulation across areas in the water with no returns. Insufficiently mapped areas were identified by triangulating bathymetric bottom points with an edge length maximum of 4.56 meters. This ensured all areas of no returns (> 9 m^2), were identified as data voids. Overall, QSI achieved successful bathymetric bottom mapping within 62.3% of the South Fork Crooked River. Of the areas successfully mapped, 79.9% had a calculated depth of 0 – 0.99 ft, 19.73% had a calculated depth of 1.00 -1.99 ft, 0.32% had a calculated depth of 2.0 – 2.99 ft, and the remaining 0.003% had a calculated depth deeper than 3.0 feet (Table 9).

Confidence

In bathymetric LiDAR collection, there are generally fewer returns at greater depths and uncertainty exists as to whether the return is actually a bottom return or part of the water column. In order to more closely assess the depths mapped, bathymetric point density at a spatial resolution of 1 m^2 was considered. The distribution of the point density within the mapped area varied depending on depth. Of the successfully mapped areas, 95.9% were mapped with high confidence containing at least 1 bathymetric classified point. The remaining 4.08% of the successfully mapped area was considered low confidence with no bathymetric classified points. These area were not considered voids due to their close proximity to surrounding bathymetric points, but contained no bathymetric point for the given cell. The confidence attribute within the mapped area shapefile provided was created based on this information.

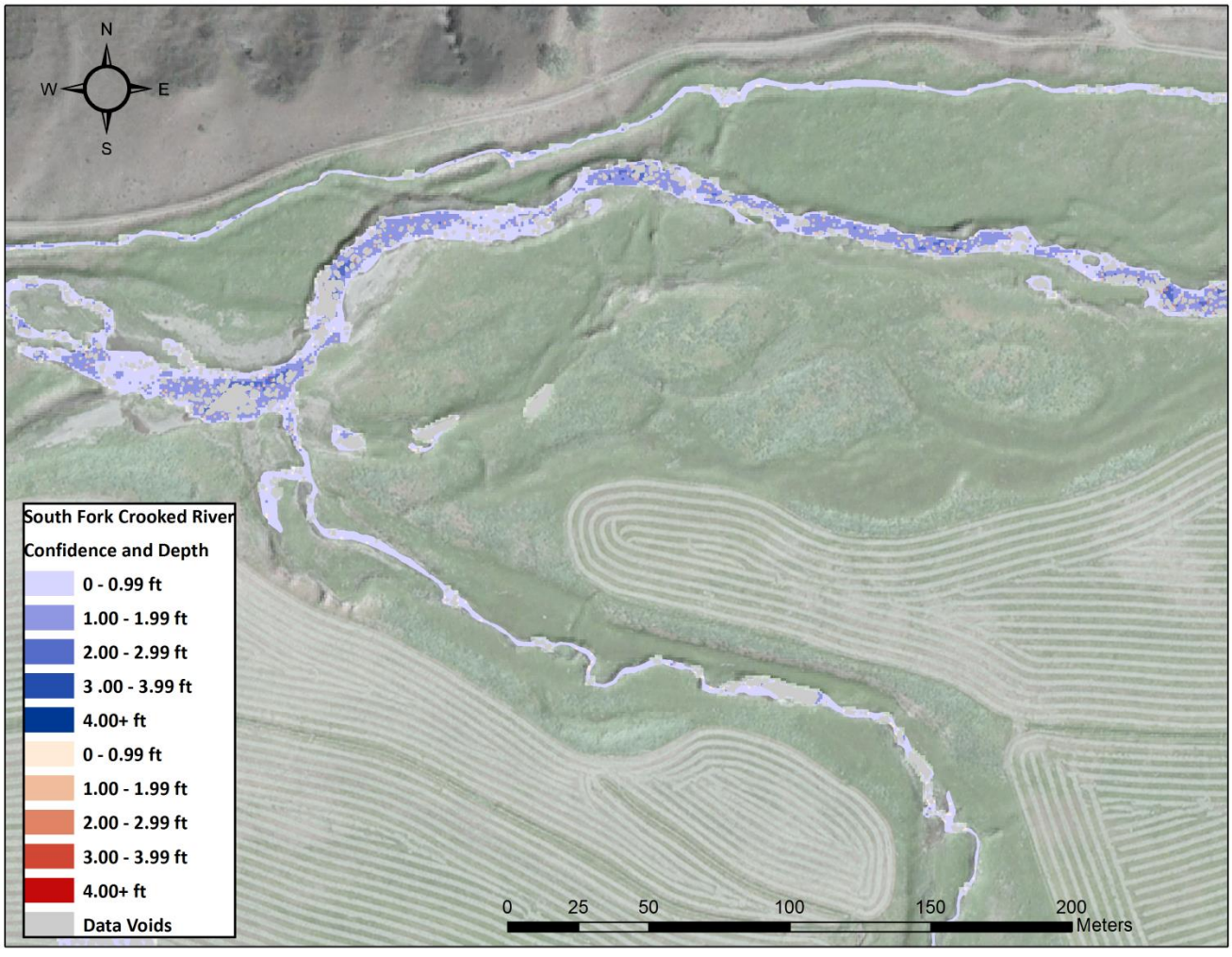

Figure 6: Sample image from the South Fork Crooked River project showing confidence values and data voids

Table 9: Summary of bathymetric bottom returns in the South Fork Crooked River

Depth Range	Percentage of Successfully Mapped Areas	Percentage Identified as High Confidence	Percentage Identified as Low Confidence
0.00 – 0.99 ft	79.90 %	96.25 %	3.75 %
1.00 – 1.99 ft	19.73 %	94.63 %	5.37 %
2.00 – 2.99 ft	0.32 %	93.37 %	6.63 %
≥ 3.00 ft	0.003 %	93.11 %	6.89 %

LiDAR Point Density

First Return Point Density

The acquisition parameters were designed to acquire an average first-return density of 5 points/m^2 for the topobathymetric AOI, and 8 points/m^2 for the NIR only AOI. First return density describes the density of pulses emitted from the laser that return at least one echo to the system. Multiple returns from a single pulse were not considered in first return density analysis. Some types of surfaces (e.g., breaks in terrain, water and steep slopes) may have returned fewer pulses than originally emitted by the laser.

With NIR LiDAR, first returns typically reflect off the highest feature on the landscape within the footprint of the pulse. In forested or urban areas the highest feature could be a tree, building or power line, while in areas of unobstructed ground, the first return will be the only echo and represents the bare earth surface.

The average first-return density of the green wavelength LiDAR data for the South Fork Crooked River project was 1.59/ft^2 (17.06 points/m^2) while the average first-return density of the NIR wavelength LiDAR data was 3.03 points/ft^2 (32.61 points/m^2) (Table 10). Within the NIR only AOI, the average first return density was 0.90 points/ft^2 (9.73 points/m^2). The statistical and spatial distributions of all first return densities per 100ft x 100ft cell are portrayed in Figure 7 through Figure 14.

Table 10: Average First Return LiDAR point densities

First Return Type	Point Density
Topobathymetric AOI Green Sensor First Returns	1.59 points/ft^2 17.06 points/m^2
Topobathymetric AOI NIR Sensor First Returns	3.03 points/ft^2 32.61 points/m^2
Topobathymetric AOI Cumulative First Returns	4.61 points/ft^2 49.67 points/m^2

First Return Type	Point Density
NIR only AOI First Returns	0.90 points/ft^2 9.73 points/m^2

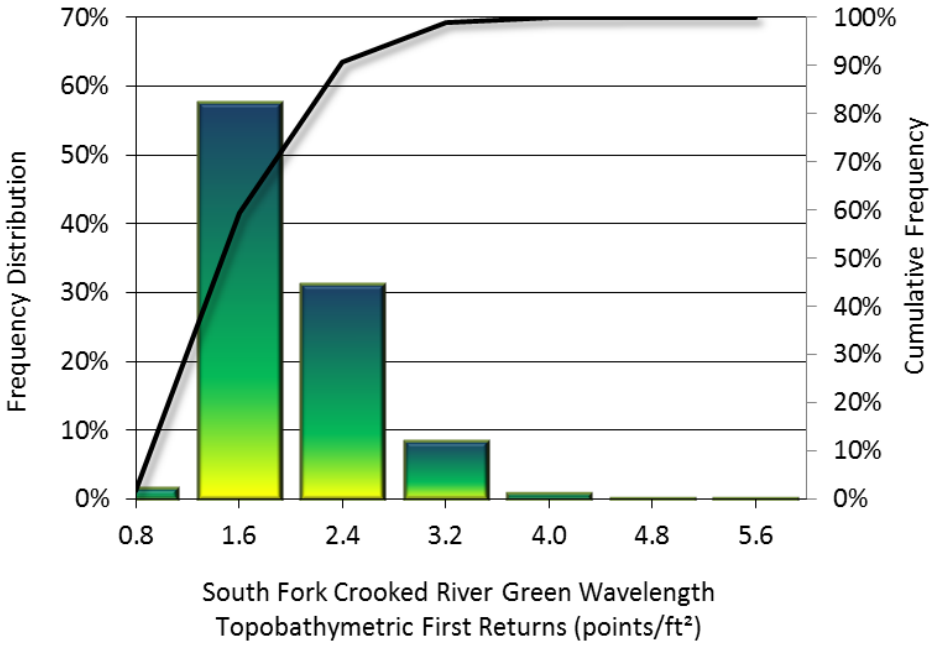

Figure 7: Frequency distribution of green wavelength first return densities per 100 x 100 ft cell

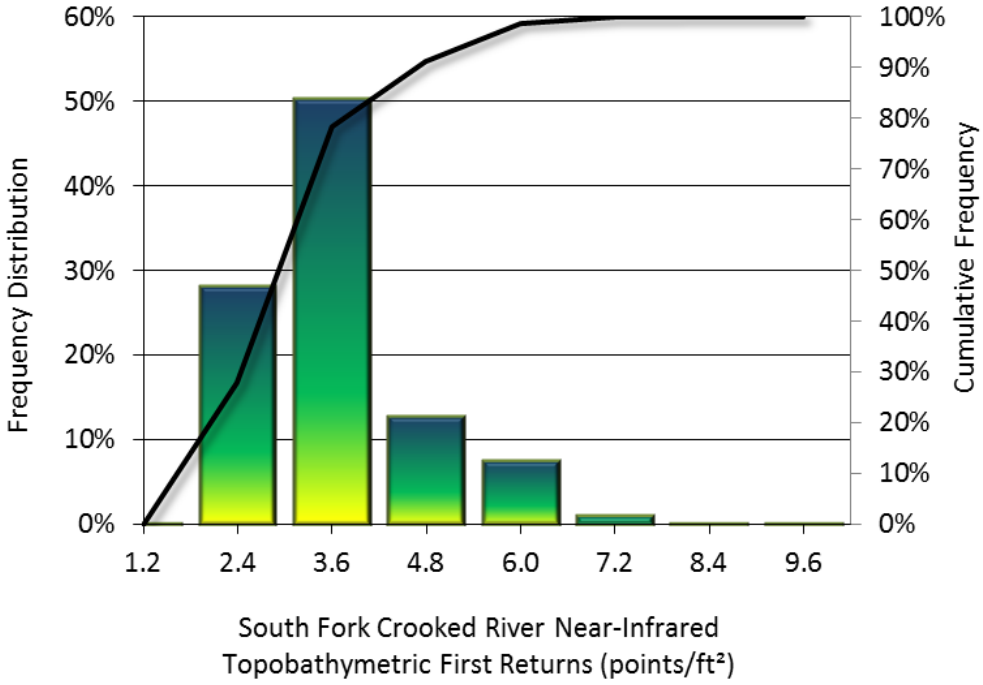

Figure 8: Frequency distribution of NIR first return densities per 100 x 100 ft cell

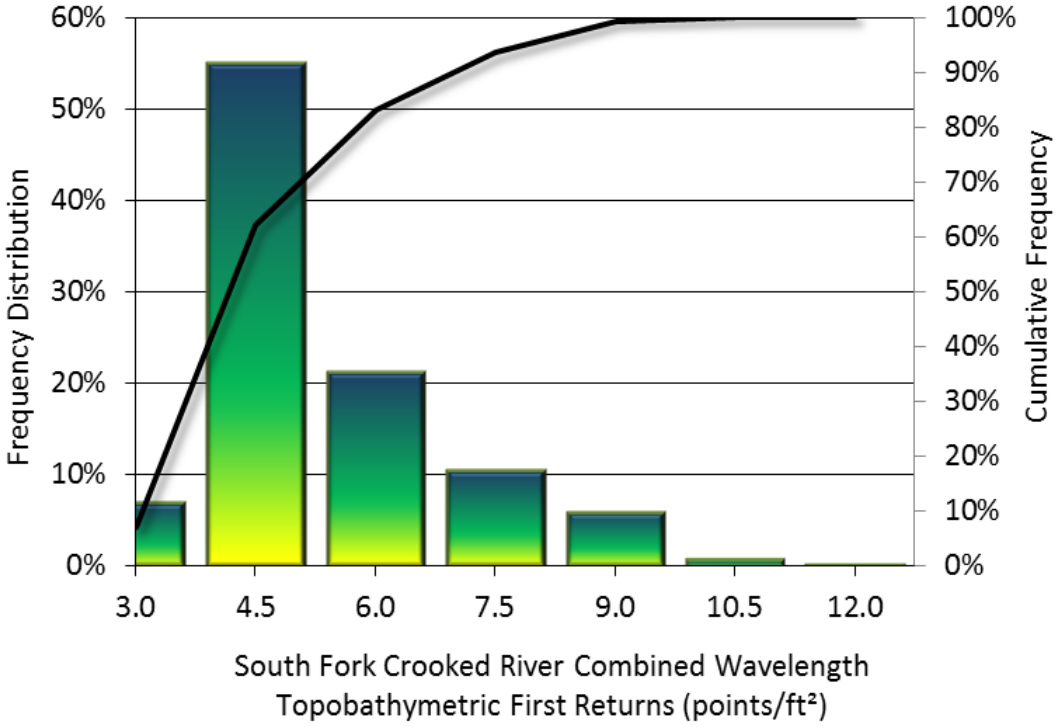

Figure 9: Frequency distribution of combined first return densities per 100 x 100 ft cell in the topobathymetric AOI

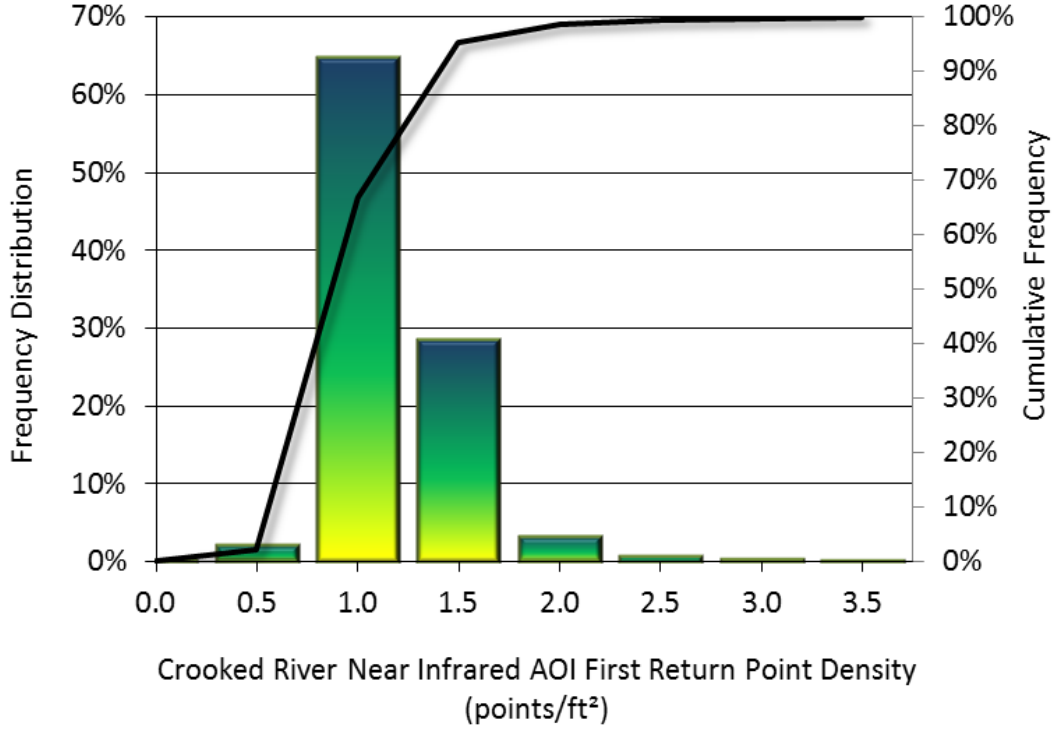

Figure 10: Frequency distribution of first return densities per 100 x 100 ft cell in the NIR AOI

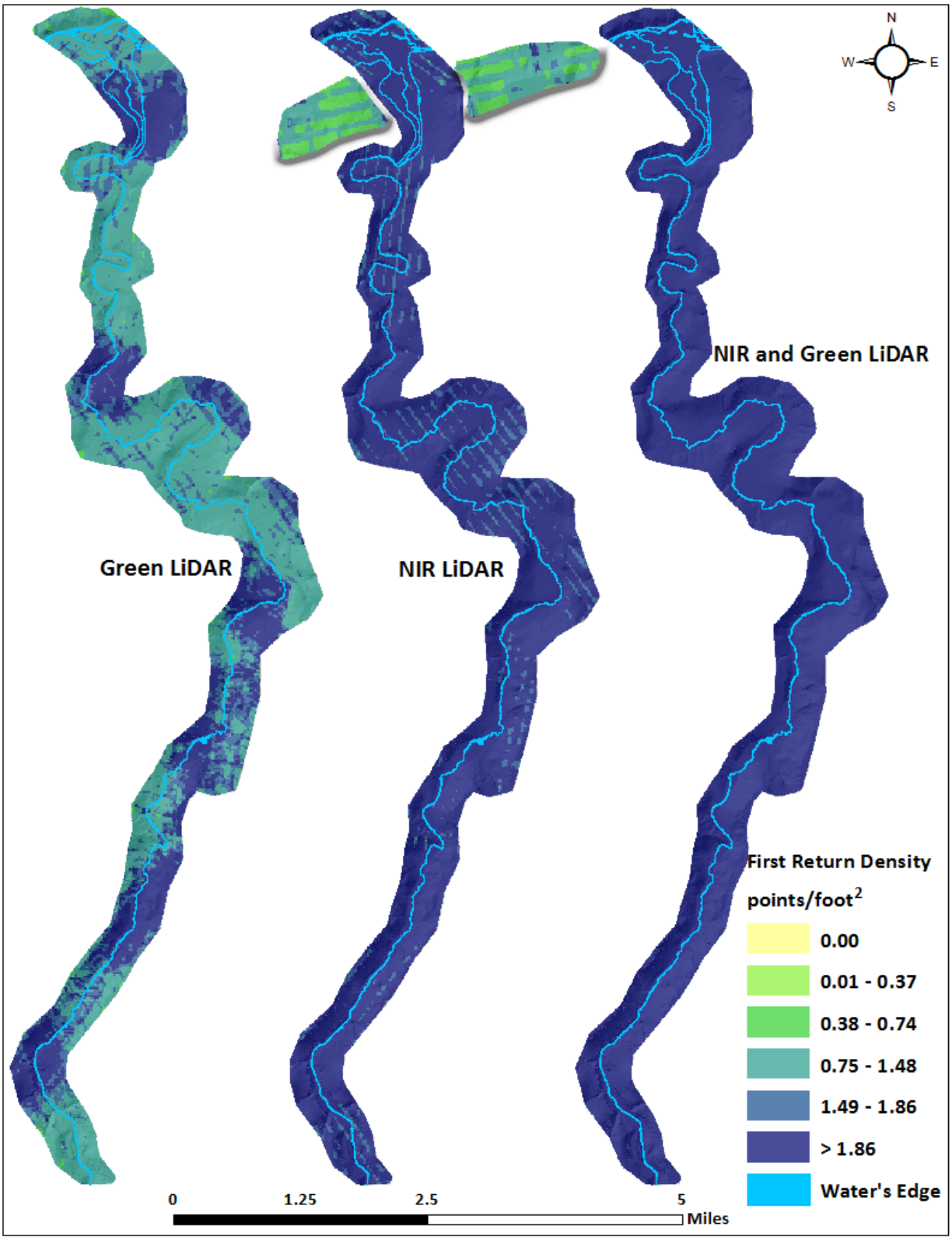

Figure 11: First return density map for the South Fork Crooked River site (100 ft x 100 ft cells)

Bathymetric and Ground Classified Point Densities

The density of ground classified LiDAR returns and bathymetric bottom returns were also analyzed for this project. Terrain character, land cover, and ground surface reflectivity all influenced the density of ground surface returns. In vegetated areas, fewer pulses may have penetrated the canopy, resulting in lower ground density. Similarly, the density of bathymetric bottom returns was influenced by turbidity, depth, and bottom surface reflectivity. In turbid areas, fewer pulses may have penetrated the water surface, resulting in lower bathymetric density.

The ground and bathymetric bottom classified density of LiDAR data for the topobathymetric AOI was 0.45 points/ft^2 (4.81 points/m^2), while the ground classified density in the NIR only AOI was 0.28 points/ft^2 (3.01 points/m^2)(Table 11). The statistical and spatial distributions ground classified and bathymetric bottom return densities per 100ft x 100ft cell are portrayed in Figure 12 through Figure 14.

Table 11: Ground Classified Point Densities

Classification	Point Density
Topobathy AOI Ground Classified Returns[3]	0.45 points/ft^2 4.81 points/m^2
NIR only AOI Ground Classified Returns	0.28 points/ft^2 3.01 points/m^2

[3] Areas lacking bathymetric returns (voids, see Figure 6) were not considered in calculating an average density value.

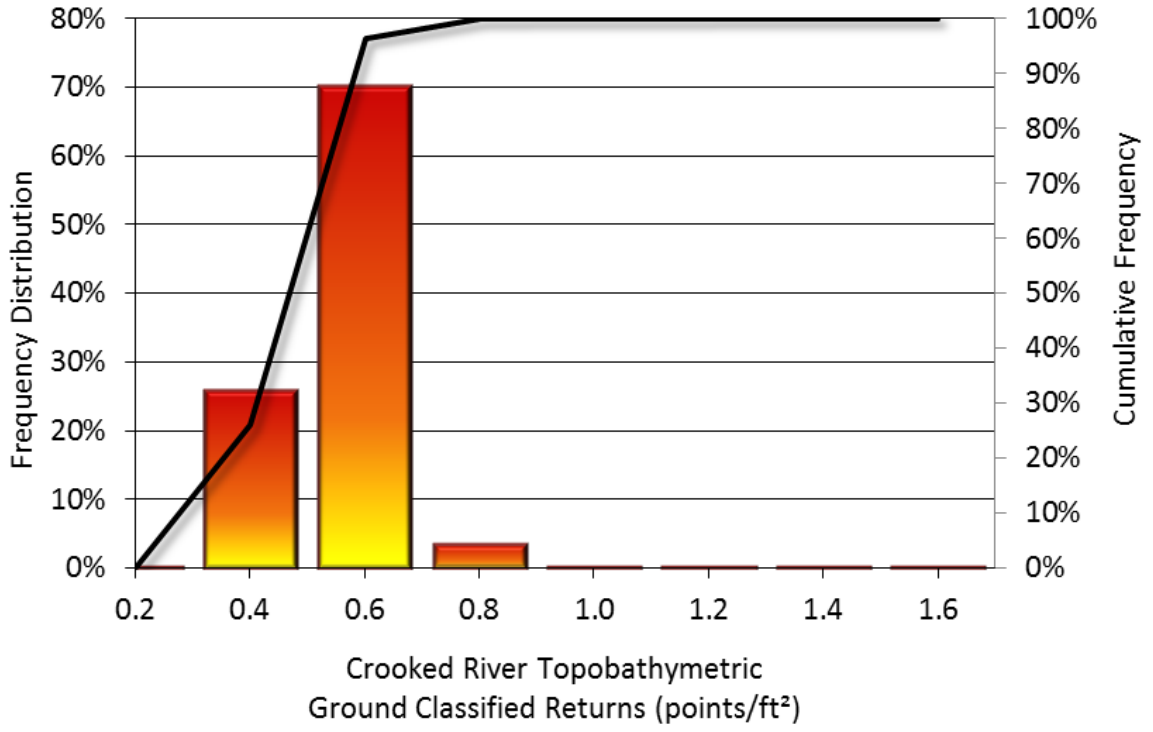

Figure 12: Frequency distribution of topobathymetric ground classified densities per 100 x 100 ft cell

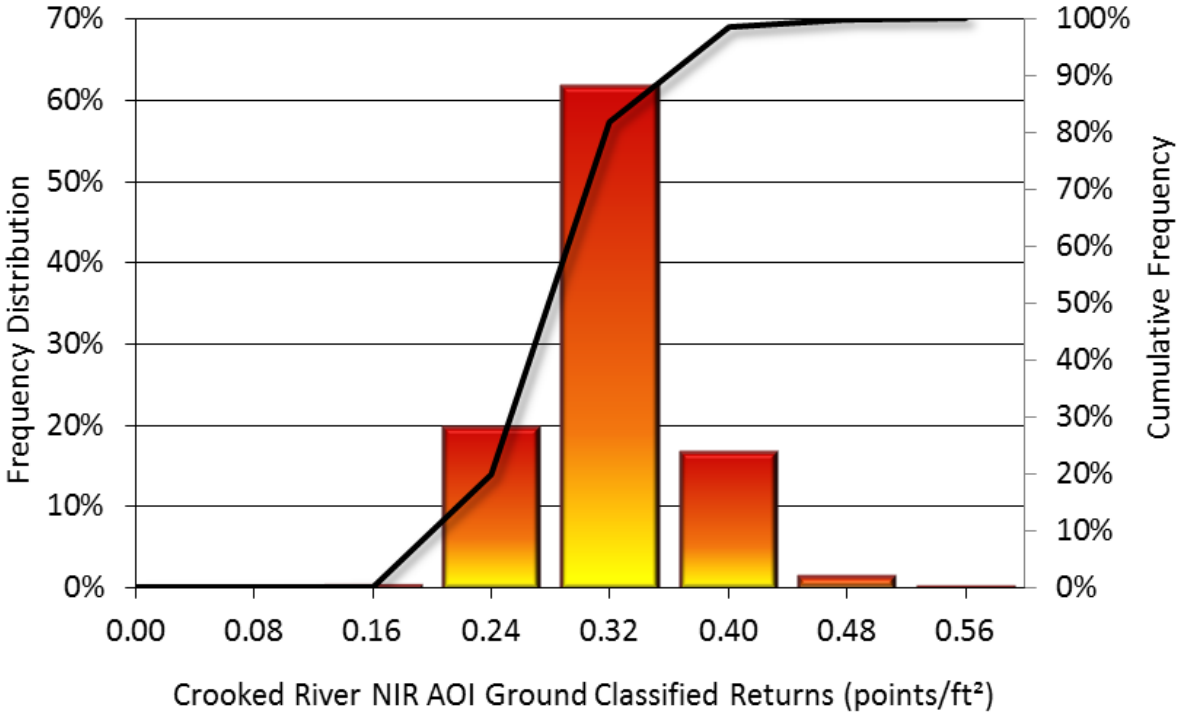

Figure 13: Frequency distribution of ground classified densities per 100 x 100 ft cell in the NIR AOI

Figure 14: Ground density map for the South Fork Crooked River site (100 ft x 100 ft cells)

LiDAR Accuracy Assessments

The accuracy of the LiDAR data collection can be described in terms of absolute accuracy (the consistency of the data with external data sources) and relative accuracy (the consistency of the dataset with itself). See Appendix A for further information on sources of error and operational measures used to improve relative accuracy.

LiDAR Absolute Accuracy

Absolute accuracy was assessed using Fundamental Vertical Accuracy (FVA) reporting designed to meet guidelines presented in the FGDC National Standard for Spatial Data Accuracy[4]. FVA compares known RTK ground check point data collected on open, bare earth surfaces with level slope (<20°) to the triangulated surface generated by the LiDAR points. FVA was assessed using ground check points for both the NIR only AOI, as well as the Topobathymetric AOI. FVA is a measure of the accuracy of LiDAR point data in open areas where the LiDAR system has a high probability of measuring the ground surface and is evaluated at the 95% confidence interval (1.96 * RMSE), as shown in Table 12. Additionally, bathymetric (submerged or along the water's edge), check points were also collected in order to assess the submerged surface vertical accuracy.

The mean and standard deviation (sigma σ) of divergence of the ground surface model from ground survey point coordinates are also considered during accuracy assessment. These statistics assume the error for x, y and z is normally distributed, and therefore the skew and kurtosis of distributions are also considered when evaluating error statistics. For the South Fork Crooked River topobathymetric survey, 19 ground check points were collected in total resulting in a fundamental vertical accuracy of 0.170 feet (0.052 meters) (Figure 15). For the South Fork Crooked River NIR only survey, 20 ground check points were collected, resulting in a fundamental vertical accuracy of 0.116 feet (0.035 meters) (Table 12).

Table 12: Absolute accuracy

Absolute Accuracy			
	Topobathymetric AOI ground check points	**NIR only AOI ground check points**	**Bathymetric check points**
Sample	19 points	20 points	41 points
FVA (1.96*RMSE)	0.170 ft 0.052 m	0.116 ft 0.035 m	0.365 ft 0.111 m
Average	0.019 ft 0.006 m	0.017 ft 0.005 m	0.024 ft 0.007 m
Median	0.023 ft 0.007 m	0.016 ft 0.005 m	0.030 ft 0.009 m
RMSE	0.087 ft 0.027 m	0.059 ft 0.018 m	0.186 ft 0.057 m

[4] Federal Geographic Data Committee, Geospatial Positioning Accuracy Standards (FGDC-STD-007.3-1998). Part 3: National Standard for Spatial Data Accuracy. http://www.fgdc.gov/standards/projects/FGDC-standards-projects/accuracy/part3/chapter3

Absolute Accuracy			
Standard Deviation (1σ)	0.087 ft 0.027 m	0.058 ft 0.018 m	0.187 ft 0.057 m

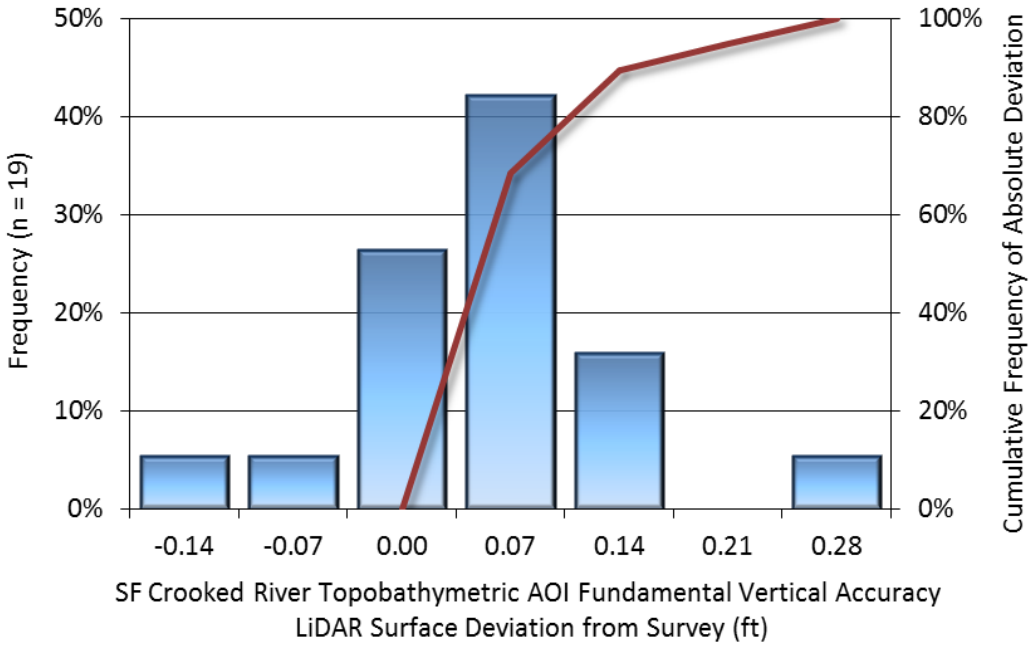

Figure 15: Frequency histogram for topobathymetric LiDAR surface deviation from ground check point values

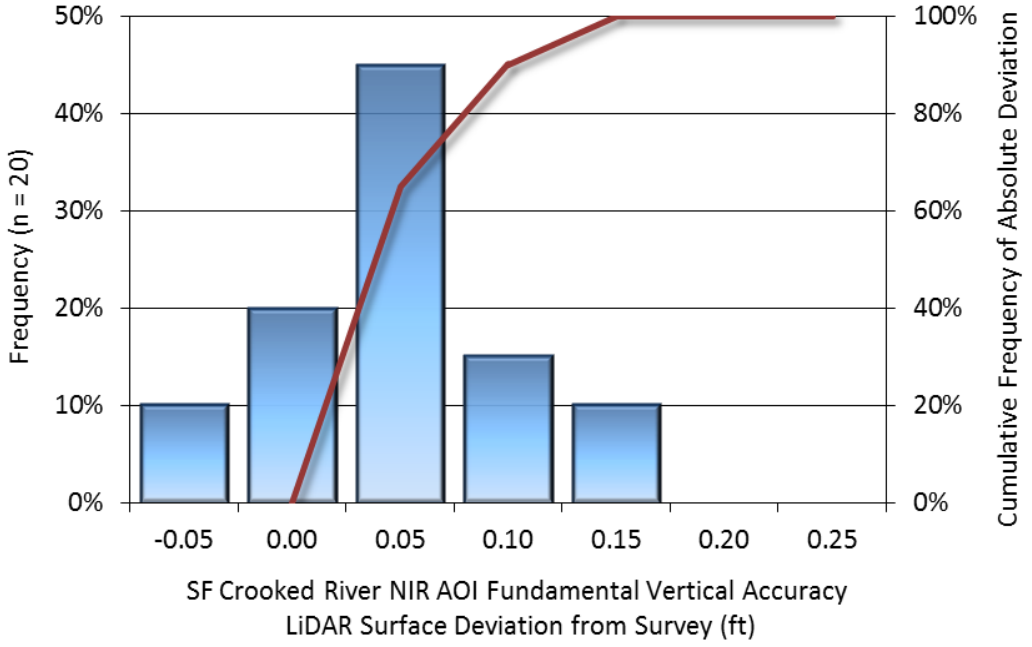

Figure 16: Frequency histogram for NIR AOI LiDAR surface deviation from ground check point values

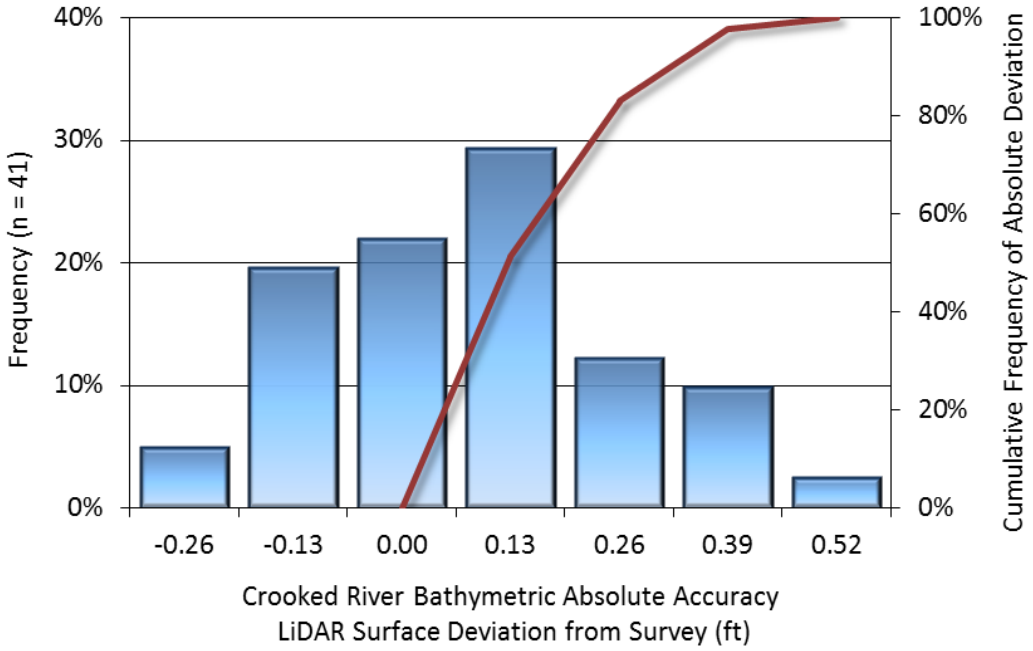

Figure 17: Frequency histogram for LiDAR bathymetric surface deviation from bathymetric check point values

LiDAR Vertical Relative Accuracy

Relative vertical accuracy refers to the internal consistency of the data set as a whole: the ability to place an object in the same location given multiple flight lines, GPS conditions, and aircraft attitudes. When the LiDAR system is well calibrated, the swath-to-swath vertical divergence is low (<0.10 meters). The relative vertical accuracy was computed by comparing the ground surface model of each individual flight line with its neighbors in overlapping regions. The average (mean) line to line relative vertical accuracy for the South Fork Crooked River topobathymetric AOI was 0.138 feet (0.042 meters), while the relative vertical accuracy for the NIR AOI was 0.107 feet (0.033 meters) (Table 13, Figure 18).

Table 13: Relative accuracy

Relative Accuracy		
	Topobathymetric AOI	**NIR only AOI**
Sample	144 surfaces	6 surfaces
Average	0.138 ft 0.042 m	0.107 ft 0.033 m
Median	0.134 ft 0.041 m	0.105 ft 0.032 m
RMSE	0.142 ft 0.043 m	0.107 ft 0.033 m

Relative Accuracy		
Standard Deviation (1σ)	0.026 ft 0.008 m	0.004 ft 0.001 m
1.96σ	0.051 ft 0.016 m	0.008 ft 0.003 m

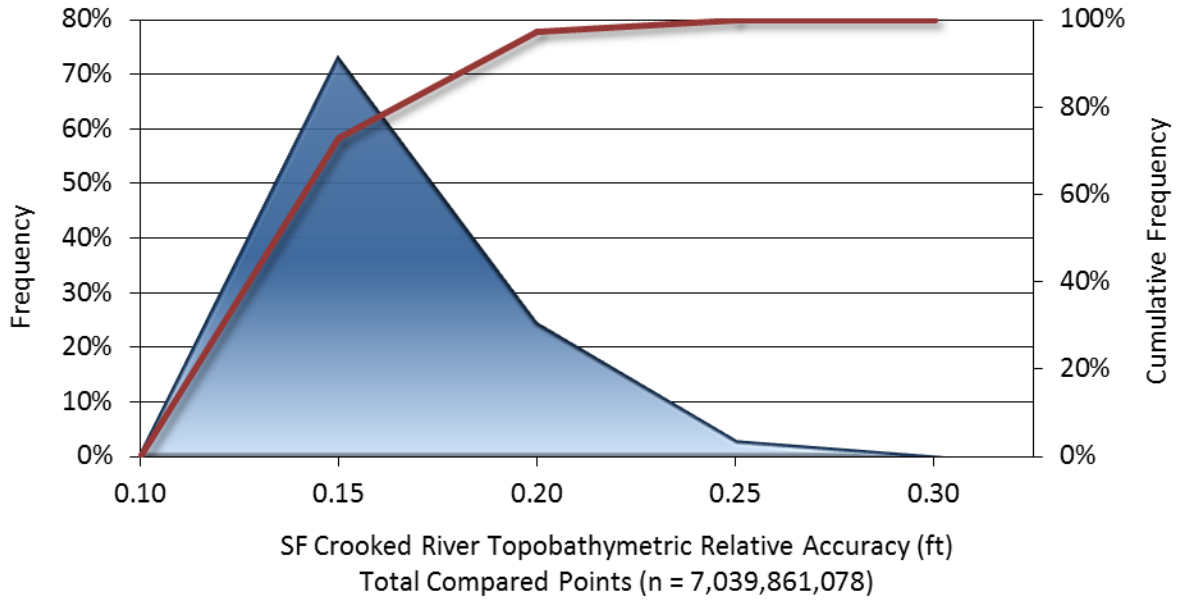

Figure 18: Frequency plot for relative vertical accuracy between flight lines in the Topobathymetric AOI

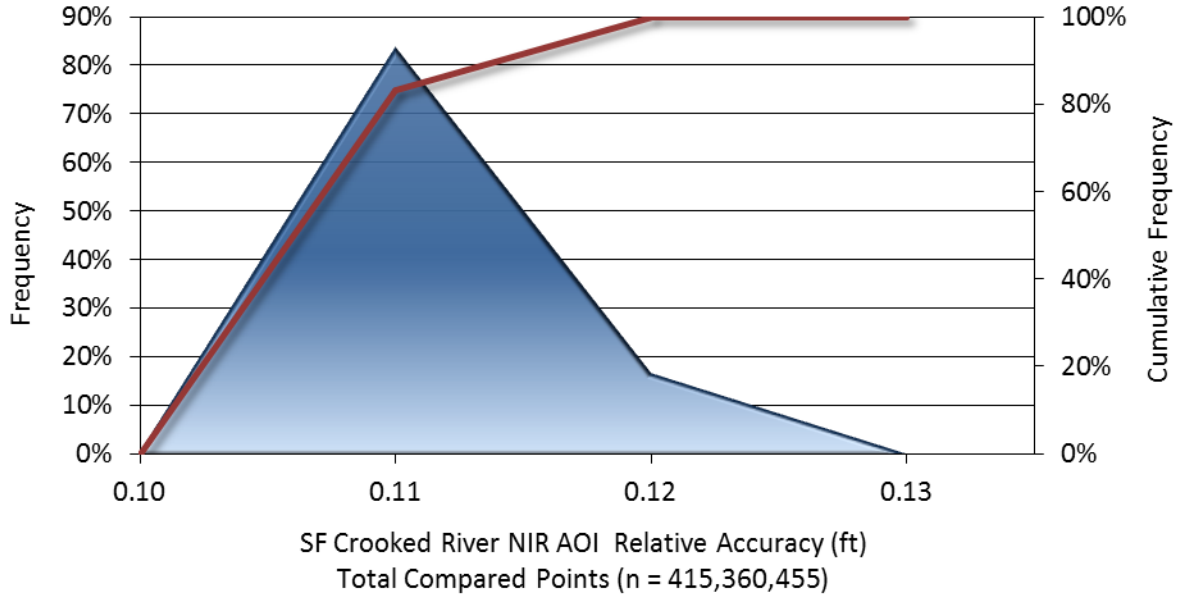

Figure 19: Frequency plot for relative vertical accuracy between flight lines in the NIR AOI

CERTIFICATIONS

Quantum Spatial provided LiDAR services for the South Fork Crooked River LiDAR project as described in this report.

I, John English, have reviewed the attached report for completeness and hereby state that it is a complete and accurate report of this project.

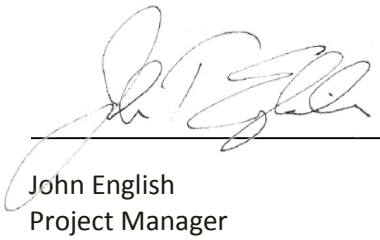

8/18/2015

John English
Project Manager
Quantum Spatial, Inc.

I, Christopher Glantz, being duly registered as a Professional Land Surveyor in and by the state of Oregon, hereby certify that the methodologies, static GNSS occupations used during airborne flights, and ground survey point collection were performed using commonly accepted Standard Practices. Field work conducted for this report was conducted between April 16, 2015 and April 17, 2015.

Accuracy statistics shown in the Accuracy Section of this Report have been reviewed by me and found to meet the "National Standard for Spatial Data Accuracy".

8/16/2015

Christopher Glantz, PLS
Professional Land Surveyor
Quantum Spatial, Inc.

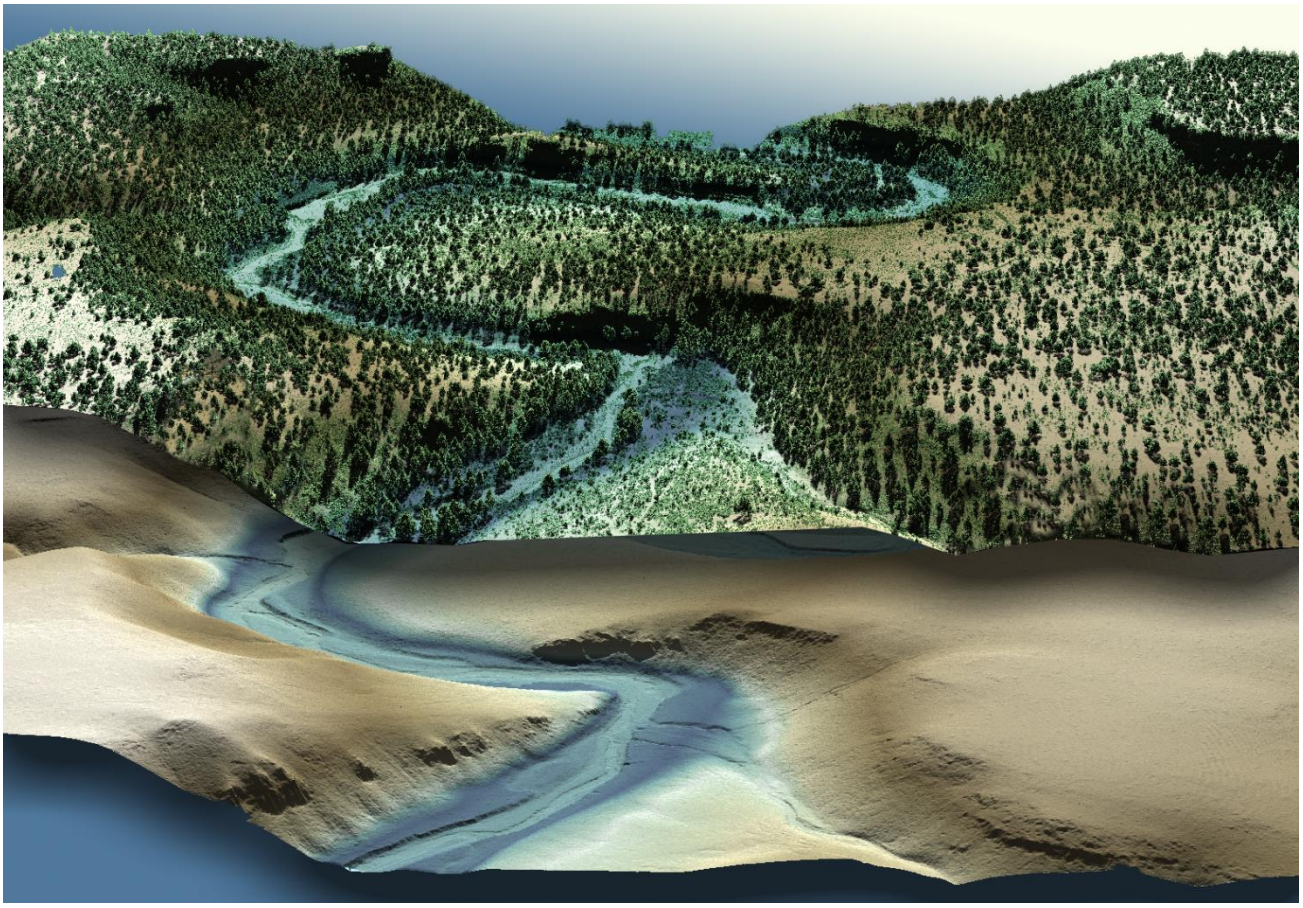

Figure 20: View looking north down Crooked River. The images were created from the gridded topobathymetric LiDAR surface colored by elevation with the 3D LiDAR point cloud overlaid in the top image.

Figure 21: View looking northwest at a towering mountain range at the northern tip of the AOI. The image was created from the gridded LiDAR surface draped with National Agriculture Imagery Program (NAIP) imagery and overlaid with the 3D LiDAR point cloud.

Figure 22: View looking southwest at a foothill south of Highway 380. The image was created from the gridded LiDAR surface colored by elevation.

GLOSSARY

1-sigma (σ) Absolute Deviation: Value for which the data are within one standard deviation (approximately 68th percentile) of a normally distributed data set.

1.96 * RMSE Absolute Deviation: Value for which the data are within two standard deviations (approximately 95th percentile) of a normally distributed data set, based on the FGDC standards for Fundamental Vertical Accuracy (FVA) reporting.

Accuracy: The statistical comparison between known (surveyed) points and laser points. Typically measured as the standard deviation (sigma σ) and root mean square error (RMSE).

> **Absolute Accuracy:** The vertical accuracy of LiDAR data is described as the mean and standard deviation (sigma σ) of divergence of LiDAR point coordinates from ground survey point coordinates. To provide a sense of the model predictive power of the dataset, the root mean square error (RMSE) for vertical accuracy is also provided. These statistics assume the error distributions for x, y and z are normally distributed, and thus we also consider the skew and kurtosis of distributions when evaluating error statistics.
>
> **Relative Accuracy:** Relative accuracy refers to the internal consistency of the data set; i.e., the ability to place a laser point in the same location over multiple flight lines, GPS conditions and aircraft attitudes. Affected by system attitude offsets, scale and GPS/IMU drift, internal consistency is measured as the divergence between points from different flight lines within an overlapping area. Divergence is most apparent when flight lines are opposing. When the LiDAR system is well calibrated, the line-to-line divergence is low (<10 cm).
>
> **Root Mean Square Error (RMSE):** A statistic used to approximate the difference between real-world points and the LiDAR points. It is calculated by squaring all the values, then taking the average of the squares and taking the square root of the average.

Data Density: A common measure of LiDAR resolution, measured as points per square meter.

Digital Elevation Model (DEM): File or database made from surveyed points, containing elevation points over a contiguous area. Digital terrain models (DTM) and digital surface models (DSM) are types of DEMs. DTMs consist solely of the bare earth surface (ground points), while DSMs include information about all surfaces, including vegetation and man-made structures.

Intensity Values: The peak power ratio of the laser return to the emitted laser, calculated as a function of surface reflectivity.

Nadir: A single point or locus of points on the surface of the earth directly below a sensor as it progresses along its flight line.

Overlap: The area shared between flight lines, typically measured in percent. 100% overlap is essential to ensure complete coverage and reduce laser shadows.

Pulse Rate (PR): The rate at which laser pulses are emitted from the sensor; typically measured in thousands of pulses per second (kHz).

Pulse Returns: For every laser pulse emitted, the number of wave forms (i.e., echos) reflected back to the sensor. Portions of the wave form that return first are the highest element in multi-tiered surfaces such as vegetation. Portions of the wave form that return last are the lowest element in multi-tiered surfaces.

Real-Time Kinematic (RTK) Survey: A type of surveying conducted with a GPS base station deployed over a known monument with a radio connection to a GPS rover. Both the base station and rover receive differential GPS data and the baseline correction is solved between the two. This type of ground survey is accurate to 1.5 cm or less.

Post-Processed Kinematic (PPK) Survey: GPS surveying is conducted with a GPS rover collecting concurrently with a GPS base station set up over a known monument. Differential corrections and precisions for the GNSS baselines are computed and applied after the fact during processing. This type of ground survey is accurate to 1.5 cm or less.

Scan Angle: The angle from nadir to the edge of the scan, measured in degrees. Laser point accuracy typically decreases as scan angles increase.

Native LiDAR Density: The number of pulses emitted by the LiDAR system, commonly expressed as pulses per square meter.

Relative Accuracy Calibration Methodology:

Manual System Calibration: Calibration procedures for each mission require solving geometric relationships that relate measured swath-to-swath deviations to misalignments of system attitude parameters. Corrected scale, pitch, roll and heading offsets were calculated and applied to resolve misalignments. The raw divergence between lines was computed after the manual calibration was completed and reported for each survey area.

Automated Attitude Calibration: All data were tested and calibrated using TerraMatch automated sampling routines. Ground points were classified for each individual flight line and used for line-to-line testing. System misalignment offsets (pitch, roll and heading) and scale were solved for each individual mission and applied to respective mission datasets. The data from each mission were then blended when imported together to form the entire area of interest.

Automated Z Calibration: Ground points per line were used to calculate the vertical divergence between lines caused by vertical GPS drift. Automated Z calibration was the final step employed for relative accuracy calibration.

LiDAR accuracy error sources and solutions:

Type of Error	Source	Post Processing Solution
GPS (Static/Kinematic)	Long Base Lines	None
	Poor Satellite Constellation	None
	Poor Antenna Visibility	Reduce Visibility Mask
Relative Accuracy	Poor System Calibration	Recalibrate IMU and sensor offsets/settings
	Inaccurate System	None
Laser Noise	Poor Laser Timing	None
	Poor Laser Reception	None
	Poor Laser Power	None
	Irregular Laser Shape	None

Operational measures taken to improve relative accuracy:

Low Flight Altitude: Terrain following was employed to maintain a constant above ground level (AGL). Laser horizontal errors are a function of flight altitude above ground (about 1/3000th AGL flight altitude).

Focus Laser Power at narrow beam footprint: A laser return must be received by the system above a power threshold to accurately record a measurement. The strength of the laser return (i.e., intensity) is a function of laser emission power, laser footprint, flight altitude and the reflectivity of the target. While surface reflectivity cannot be controlled, laser power can be increased and low flight altitudes can be maintained.

Reduced Scan Angle: Edge-of-scan data can become inaccurate. The scan angle was reduced to a maximum of ±15^{o} from nadir, creating a narrow swath width and greatly reducing laser shadows from trees and buildings.

Quality GPS: Flights took place during optimal GPS conditions (e.g., 6 or more satellites and PDOP [Position Dilution of Precision] less than 3.0). Before each flight, the PDOP was determined for the survey day. During all flight times, a dual frequency DGPS base station recording at 1 second epochs was utilized and a maximum baseline length between the aircraft and the control points was less than 13 nm at all times.

Ground Survey: Ground survey point accuracy (<1.5 cm RMSE) occurs during optimal PDOP ranges and targets a minimal baseline distance of 4 miles between GPS rover and base. Robust statistics are, in part, a function of sample size (n) and distribution. Ground survey points are distributed to the extent possible throughout multiple flight lines and across the survey area.

50% Side-Lap (100% Overlap): Overlapping areas are optimized for relative accuracy testing. Laser shadowing is minimized to help increase target acquisition from multiple scan angles. Ideally, with a 50% side-lap, the nadir portion of one flight line coincides with the swath edge portion of overlapping flight lines. A minimum of 50% side-lap with terrain-followed acquisition prevents data gaps.

Opposing Flight Lines: All overlapping flight lines have opposing directions. Pitch, roll and heading errors are amplified by a factor of two relative to the adjacent flight line(s), making misalignments easier to detect and resolve.